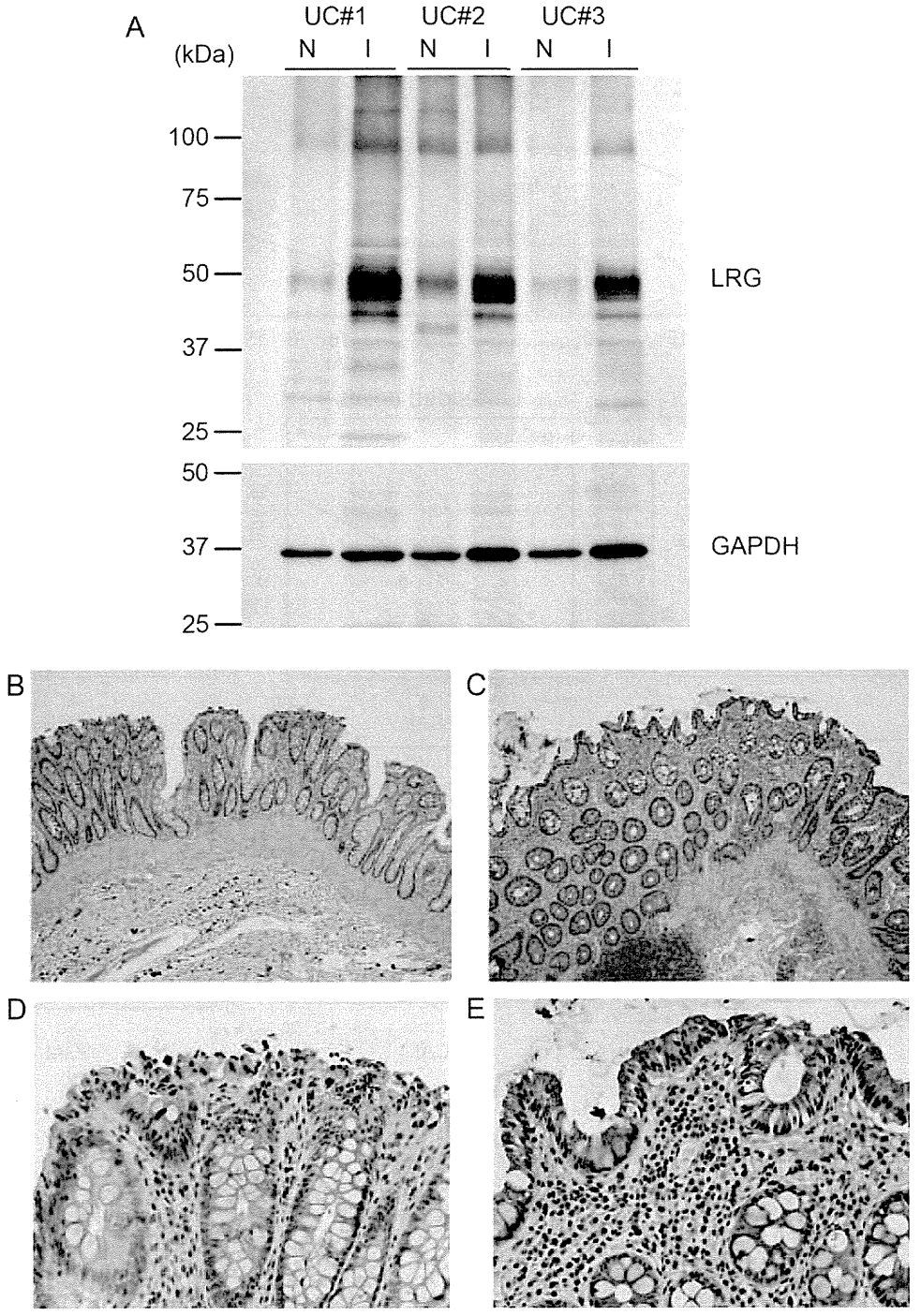

FIGURE 3. Expression of LRG is increased in lesion sites of ulcerative colitis. (A) Representative western blot analysis of three separate experiments for LRG using paired surgically resected full-thickness colon specimens from noninflamed (N) and inflamed (I) sites in patients with UC. GAPDH was used as a control of the relative amounts of proteins in each sample. Full-thickness colon tissues from UC in inflamed and noninflamed sites were evaluated by immunohistochemical analysis for LRG expression ($n = 10$ per experimental group). (B) Noninflamed mucosa (×42). (C) Inflamed mucosa from active UC (×42). (D) Noninflamed mucosa (×400). (E) Inflamed mucosa from active UC (×400).

to be increased at the inflamed tissue in active UC.[24–26] Indeed, ELISA analysis using sera from 82 UC patients revealed that serum TNF-α, IL-6, and IL-22 levels were significantly elevated in active UC patients compared with those patients in remission ($P = 0.0178$, $P = 0.00690$, and $P < 0.0001$, respectively) (Fig. 4A). Next, to investigate

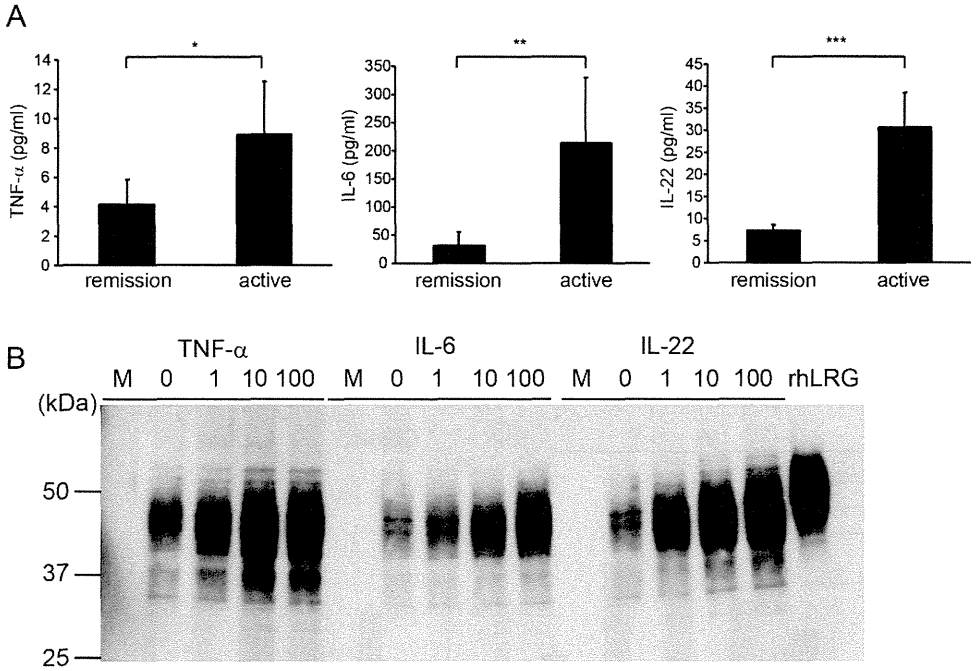

FIGURE 4. Expression of LRG was induced by TNF-α, IL-6, and IL-22. (A) Serum levels of TNF-α, IL-6, and IL-22 were determined in patients with UC (57 patients in remission [CAI <6] and 25 patients in active [CAI ≥6] stage). Data are expressed as mean ± SEM. *$P < 0.05$, **$P < 0.005$, ***$P < 0.0001$ by Mann–Whitney U-test. (B) LRG was determined in supernatants of COLO205 cells left untreated or stimulated with TNF-α, IL-6, and IL-22 at 1.0, 10, 100 ng/mL for 24 hours and analyzed by western blotting. There was a dose-dependent increase in LRG levels after treatment with TNF-α, IL-6, and IL-22.

which proinflammatory cytokines induce expression of LRG we stimulated human colonic adenocarcinoma COLO205 cells with TNF-α, IL-6, or IL-22 for 24 hours. After cytokine stimulation, secretion of LRG protein into the culture media was analyzed by western blotting. Interestingly, LRG was induced not only by stimulation with IL-6, but also by TNF-α and IL-22 in a dose-dependent manner (Fig. 4B). These results indicate that expression of LRG is induced by various proinflammatory cytokines including IL-6.

Expression of LRG Through an IL-6-independent Pathway Is Demonstrated in LPS-mediated Acute Inflammation and DSS-induced Colitis

CRP is one of the representative acute phase proteins in humans and CRP production is primarily dependent on liver by circulating IL-6. To examine the possible differences in induction mechanisms between LRG and CRP, particularly with regard to the involvement of IL-6, we took advantage of murine models. We first assessed whether LRG is induced in WT mice by injecting LPS, an inducer of proinflammatory cytokines from macrophages, because CRP is poorly induced in mice during acute inflammation. At 24 hours after intraperitoneal injection of LPS, serum samples were prepared and serum LRG levels were determined by ELISA. Compared with WT mice, significant elevation of serum LRG levels were detected in LPS-administered WT mice (Fig. 5A), suggesting that LRG is induced during acute inflammation in mice as in humans.

We next used a murine IBD model to investigate induction mechanisms of LRG during colonic inflammation. DSS-induced colitis is often used as a murine model of UC.[27] We induced colitis in WT mice by treating them with 3% DSS for 5 days and measured changes in relative body weight. Body weight began to decrease at day 5, showed greatest reduction at day 9, and recovered at 18 days after DSS treatment (Fig. 5B). We analyzed changes in serum LRG levels by ELISA before and 5, 7, 10, 15, and 25 days after DSS treatment. Consistent with body weight loss, serum LRG levels were significantly elevated at 5 days after DSS treatment (Fig. 5C). Serum LRG levels remained high until day 15, but decreased at day 25. Delayed normalization of serum LRG levels is likely due to the prolonged inflammation at inflamed tissue sites. Additionally, a long half-life of serum LRG might also be involved in this, since our preliminary data suggest that the half-life of serum human LRG levels are about two times longer than that of CRP (data not shown). To investigate which organs produce LRG in DSS-induced colitis, RNA was extracted from colon, liver, and spleen before and 9 days after DSS treatment. By quantitative PCR analysis (Fig. 5D), expression of LRG was significantly increased in liver ($P = 0.00106$) and spleen ($P = 0.0376$);

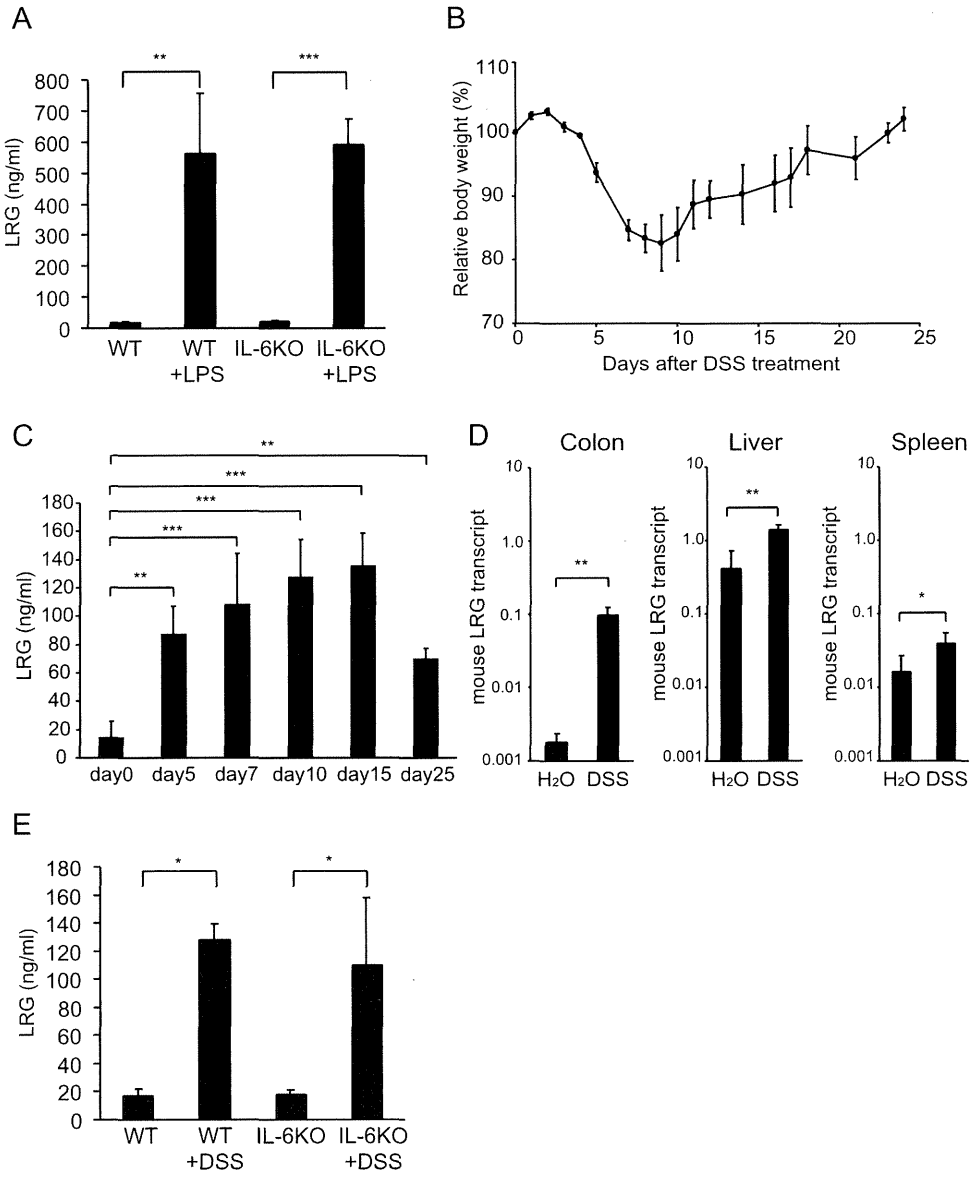

FIGURE 5. Induction of LRG has IL-6-independent pathway in LPS-mediated acute inflammation and active stage of DSS-induced colitis. (A) WT mice and IL-6-deficient mice were injected intraperitoneally with 0 or 10 mg/kg LPS dissolved in 500 μL PBS and serum LRG levels were measured after 24 hours. Data are expressed as mean ± SEM. $^{**}P < 0.005$, $^{***}P < 0.0001$ by one-way ANOVA followed by Scheffe's post-hoc test. (B) Relative body weight changes of mice with DSS-induced colitis in this study. Data are expressed as mean ± SEM ($n = 4$). (C) Expression of LRG is upregulated in murine DSS-induced colitis. At the indicated time, serum LRG levels were determined by ELISA analysis. $^{**}P < 0.005$, $^{***}P < 0.0001$ by one-way ANOVA followed by a by Dunnett's post-hoc test. (D) Nine days after control or DSS treatment, mice were euthanized and gene expression of LRG in the colon, liver, spleen, and kidney was determined by quantitative PCR analysis. Gene expression was calculated relative to HPRT. Data were expressed as mean ± SD ($n = 5$). $^{*}P < 0.05$, $^{**}P < 0.005$ by Student's t-test. (E) IL-6-deficient mice were used for DSS-induced colitis. Nine days after DSS administration, serum levels of mouse LRG was determined by ELISA analysis. $^{*}P < 0.05$ by one-way ANOVA followed by Scheffe's post-hoc test.

however, the strongest induction was observed in colon ($P = 0.000126$).

To investigate whether LRG induction is dependent on IL-6 or not, we analyzed serum LRG levels in IL-6-deficient mice. Interestingly, basal LRG levels in IL-6-deficient mice were similar to those in WT mice and LRG was robustly induced by LPS administration in IL-6-deficient mice (Fig. 5A). Moreover, increased serum LRG levels were also detected in the active stage (day 9) of DSS-induced colitis in IL-6-deficient mice (Fig. 5E). Importantly, the increase of serum LRG in IL-6-deficient mice was similar to that in WT mice (Fig. 5A,E). These findings indicate that LRG expression can be induced in the absence of IL-6.

DISCUSSION

In this study we first demonstrated that serum LRG levels were significantly increased in sera of active UC patients compared with patients in remission and HC. Serum LRG is likely elevated in diverse racial groups, because we detected increased serum LRG levels not only in Japanese patients (Fig. 1A)[13] but also in Caucasian patients with UC (Fig. 1C,D) and CD (data not shown). In addition, levels of serum LRG were significantly correlated with disease activity in UC and the correlation was stronger than CRP. Moreover, by analyzing ROC curve and AUC, serum LRG levels showed higher AUC than CRP and serum LRG levels represented superior sensitivity and specificity to CRP for remission and active of UC by CAI (Fig. 2D), indicating that LRG is a useful marker to evaluate disease activity in UC. In the normal state, serum LRG is thought to be produced from liver and LRG is abundantly found in the sera of HC. In colonic inflammation, we found that the expression of LRG is increased in the inflamed mucosa of UC patients and mice with DSS colitis, suggesting that inflamed tissues can be a source for production of LRG (Fig. 3). The increased expression of LRG in inflamed tissue has previously been observed in appendix during acute appendicitis.[28] Moreover, in acute inflammatory disorders, including appendicitis and diverticulitis, increased expression of serum LRG was observed (Fig. 1A). These results indicate that the elevated expression of LRG at inflamed sites and in sera occurs in various acute and chronic inflammatory disorders. Therefore, increased serum LRG levels are not suitable for use as a specific diagnostic marker of IBD.

CRP is the most common serum marker used to evaluate disease activity in inflammatory diseases. However, serum CRP is primarily dependent on liver production induced by circulating IL-6. Compared with CD and RA, only modest to absent CRP responses are observed in UC, despite active inflammation in colon.[9] Indeed, our cohort of 82 UC patients, analyzed in this study, included five patients with normal value of CRP while having active disease (Fig. 2A). However, our study demonstrated that serum LRG levels were significantly increased in active UC patients' sera and correlated better with disease activity of UC than CRP levels (Figs. 1A, 2A). Particularly, in the group of patients with negative CRP (CRP <0.2), significant correlation was observed between serum LRG levels and CAI (Supporting Fig. 2C). Similarly, among CRP-negative patients serum LRG levels were significantly elevated in those with endoscopically active UC, compared with UC in remission (Supporting Fig. 1B). In addition, serum LRG levels were decreased after therapy (Fig. 2C), suggesting that LRG is a useful serological biomarker for evaluating disease activity and therapeutic effect in UC.

Better correlation of serum LRG levels with disease activity of UC than CRP might be explained in part by the differences in induction mechanisms between LRG and CRP. While the expression of CRP is essentially dependent on IL-6, several cytokines may compensate for the absence of elevated IL-6 in induction of LRG expression. Accordingly, expression of LRG in COLO205 cells was induced not only by IL-6 but also by TNF-α and IL-22 (Fig. 4B), all of which were increased in sera of UC patients (Fig. 4A). Expression of LRG was strongly induced by IL-22 in COLO205 cells, correlating with enhanced STAT3 (Tyr705) phosphorylation by IL-22 compared with IL-6 (data not shown). Thus, inflammatory cytokines such as TNF-α and IL-22 may mediate LRG expression in the absence of IL-6. Moreover, using DSS-induced colitis in IL-6-deficient mice we could demonstrate an IL-6-independent pathway for LRG induction (Fig. 5E). Because promoter regions of human and mouse LRG share high sequence homology and contain putative binding sites for transcription factors such as C/EBP, MZF1, and STAT,[17] it is conceivable that the similar IL-6-independent mechanisms of LRG induction are also involved in humans. Future studies are required to fully elucidate the induction mechanisms of LRG in both humans and mice.

In the three disease categories of UC based on extent of disease, serum LRG levels tended to be low in proctitis compared with extensive colitis and left-sided colitis (Fig. 1B). In addition, correlation between serum LRG levels and disease activity did not reach significance in proctitis (Fig. 2B). Although the low number of patients with active proctitis may preclude the proper evaluation of LRG levels, limited inflamed area of proctitis may also be a reason for slight increases of serum LRG levels in these patients. Given the increased production of LRG in inflamed colonic mucosa, fecal LRG might be a more sensitive disease biomarker for UC including proctitis. Optimization for the measurement of fecal LRG is currently under way in our laboratory.

This study also highlights the potential usefulness of LRG in evaluating murine colitis. Our results indicate that serum LRG levels increase as the disease progresses in a DSS-induced colitis model (Fig. 5B,C). In addition, the LRG expression is significantly upregulated in the colon with DSS-induced colitis (Fig. 5D). Thus, LRG in mice can be an objective disease activity marker for colitis models and may be useful for preclinical studies of IBD.

In conclusion, serum LRG levels reflect disease activity of UC better than CRP, especially in patients with low CRP. In the inflammatory condition, LRG is expressed in the inflamed tissue and expression of LRG is regulated by mechanisms different from that of CRP. These findings suggest that serum LRG is a novel and potential serologic biomarker for evaluating disease activity of UC.

ACKNOWLEDGMENTS

We thank T. Mizushima for provision of appendicitis and diverticulitis patients' sera, Y. Kanazawa for secretarial

assistance, and M. Urase and A. Morimoto for technical assistance.

REFERENCES

1. Nikolaus S, Schreiber S. Diagnostics of inflammatory bowel disease. *Gastroenterology*. 2007;133:1670–1689.
2. Baumgart DC, Sandborn WJ. Inflammatory bowel disease: clinical aspects and established and evolving therapies. *Lancet*. 2007;369: 1641–1657.
3. Stange EF, Travis SP, Vermeire S, et al. European evidence based consensus on the diagnosis and management of Crohn's disease: definitions and diagnosis. *Gut*. 2006;55(Suppl 1):i1–15.
4. Caprilli R, Viscido A, Latella G. Current management of severe ulcerative colitis. *Nat Clin Pract Gastroenterol Hepatol*. 2007;4:92–101.
5. Kornbluth A, Sachar DB. Ulcerative colitis practice guidelines in adults (update): American College of Gastroenterology, Practice Parameters Committee. *Am J Gastroenterol*. 2004;99:1371–1385.
6. Sands BE, Abreu MT, Ferry GD, et al. Design issues and outcomes in IBD clinical trials. *Inflamm Bowel Dis*. 2005;11(Suppl 1):S22–28.
7. Freeman HJ. Use of the Crohn's disease activity index in clinical trials of biological agents. *World J Gastroenterol*. 2008;14:4127–4130.
8. Best WR, Becktel JM, Singleton JW, et al. Development of a Crohn's disease activity index. National Cooperative Crohn's Disease Study. *Gastroenterology*. 1976;70:439–444.
9. Vermeire S, Van Assche G, Rutgeerts P. C-reactive protein as a marker for inflammatory bowel disease. *Inflamm Bowel Dis*. 2004;10: 661–665.
10. Pepys MB, Druguet M, Klass HJ, et al. Immunological studies in inflammatory bowel disease. *Ciba Found Symp* 1977:283–304.
11. Saverymuttu SH, Hodgson HJ, Chadwick VS, et al. Differing acute phase responses in Crohn's disease and ulcerative colitis. *Gut*. 1986; 27:809–813.
12. Colombel JF, Rutgeerts P, Reinisch W, et al. Early mucosal healing with infliximab is associated with improved long-term clinical outcomes in ulcerative colitis. *Gastroenterology*. 2011;141:1194–1201.
13. Serada S, Fujimoto M, Ogata A, et al. iTRAQ-based proteomic identification of leucine-rich alpha-2 glycoprotein as a novel inflammatory biomarker in autoimmune diseases. *Ann Rheum Dis*. 2010;69:770–774.
14. Haupt H, Baudner S. Isolation and characterization of an unknown, leucine-rich 3.1-S-alpha2-glycoprotein from human serum [author's transl]. *Hoppe Seylers Z Physiol Chem*. 1977;358:639–646.
15. Takahashi N, Takahashi Y, Putnam FW. Periodicity of leucine and tandem repetition of a 24-amino acid segment in the primary structure of leucine-rich alpha 2-glycoprotein of human serum. *Proc Natl Acad Sci U S A*. 1985;82:1906–1910.
16. Shirai R, Hirano F, Ohkura N, et al. Up-regulation of the expression of leucine-rich alpha(2)-glycoprotein in hepatocytes by the mediators of acute-phase response. *Biochem Biophys Res Commun*. 2009;382: 776–769.
17. O'Donnell LC, Druhan LJ, Avalos BR. Molecular characterization and expression analysis of leucine-rich alpha2-glycoprotein, a novel marker of granulocytic differentiation. *J Leukoc Biol*. 2002;72: 478–485.
18. Rachmilewitz D. Coated mesalazine (5-aminosalicylic acid) versus sulphasalazine in the treatment of active ulcerative colitis: a randomised trial. *BMJ*. 1989;298:82–86.
19. Kruis W, Schreiber S, Theuer D, et al. Low dose balsalazide (1.5 g twice daily) and mesalazine (0.5 g three times daily) maintained remission of ulcerative colitis but high dose balsalazide (3.0 g twice daily) was superior in preventing relapses. *Gut*. 2001;49:783–789.
20. Matts SG. The value of rectal biopsy in the diagnosis of ulcerative colitis. *Q J Med*. 1961;30:393–407.
21. Iwahori K, Serada S, Fujimoto M, et al. Overexpression of SOCS3 exhibits preclinical antitumor activity against malignant pleural mesothelioma. *Int J Cancer*. 2011;129:1005–1017.
22. Kim A, Enomoto T, Serada S, et al. Enhanced expression of Annexin A4 in clear cell carcinoma of the ovary and its association with chemoresistance to carboplatin. *Int J Cancer*. 2009;125:2316–2322.
23. Fujimoto M, Nakano M, Terabe F, et al. The influence of excessive IL-6 production in vivo on the development and function of Foxp3+ regulatory T cells. *J Immunol*. 2011;186:32–40.
24. Murch SH, Lamkin VA, Savage MO, et al. Serum concentrations of tumour necrosis factor alpha in childhood chronic inflammatory bowel disease. *Gut*. 1991;32:913–917.
25. Woywodt A, Ludwig D, Neustock P, et al. Mucosal cytokine expression, cellular markers and adhesion molecules in inflammatory bowel disease. *Eur J Gastroenterol Hepatol*. 1999;11:267–276.
26. Andoh A, Zhang Z, Inatomi O, et al. Interleukin-22, a member of the IL-10 subfamily, induces inflammatory responses in colonic subepithelial myofibroblasts. *Gastroenterology*. 2005;129:969–984.
27. Okayasu I, Hatakeyama S, Yamada M, et al. A novel method in the induction of reliable experimental acute and chronic ulcerative colitis in mice. *Gastroenterology*. 1990;98:694–702.
28. Kentsis A, Lin YY, Kurek K, et al. Discovery and validation of urine markers of acute pediatric appendicitis using high-accuracy mass spectrometry. *Ann Emerg Med*. 2010;55:62–70 e4.

Tumor Biol. (2012) 33:1141–1149
DOI 10.1007/s13277-012-0356-9

RESEARCH ARTICLE

Serum HE4 as a diagnostic and prognostic marker for lung cancer

Kota Iwahori · Hidekazu Suzuki · Yoshiro Kishi · Yoshihiro Fujii · Rie Uehara · Norio Okamoto · Masashi Kobayashi · Tomonori Hirashima · Ichiro Kawase · Tetsuji Naka

Received: 19 December 2011 / Accepted: 9 February 2012 / Published online: 29 February 2012

Abstract We evaluated the diagnostic and prognostic efficacy of human epididymis protein 4 (HE4) for lung cancer patients by using our novel enzyme-linked immunosorbent assay (ELISA) system. We measured serum HE4 levels of cancer patients including 49 lung cancer and 18 ovarian cancer patients. Furthermore, we evaluated the relationship between serum HE4 levels and overall survival after chemotherapy of 24 lung cancer patients. Serum HE4 levels were significantly higher for non-small, small cell lung cancer and ovarian cancer patients than for healthy controls. The area under the receiver operating characteristic curve (AUC) was calculated for differentiation of lung cancer patients and healthy controls. AUC for serum HE4 was 0.988 for differentiating lung cancer patients from healthy controls, with a cutoff value of 6.56 ng/ml (sensitivity= 89.8%, specificity=100%). Serum HE4 levels were elevated in 36/40 (90.0%) non-small cell lung cancer patients, 8/9 (88.9%) small cell lung cancer patients and 8/18 (44.4%) ovarian cancer patients. High levels of serum HE4 (>15 ng/ml) after chemotherapy were significantly correlated with worse overall survival after the treatment. These findings suggest that serum HE4 is a potential diagnostic and prognostic marker for lung cancer patients.

Keywords HE4 · Tumor marker · ELISA · Lung cancer · Chemotherapy

K. Iwahori · T. Naka (✉)
Laboratory for Immune Signal,
National Institute of Biomedical Innovation,
7-6-8 Saito-Asagi,
Ibaraki, Osaka 567-0085, Japan
e-mail: tnaka@nibio.go.jp

K. Iwahori
Department of Respiratory Medicine, Allergy, and Rheumatic Diseases, Osaka University Graduate School of Medicine,
2-2 Yamada-oka,
Suita, Osaka 565-0871, Japan

H. Suzuki · N. Okamoto · M. Kobayashi · T. Hirashima · I. Kawase
Department of Thoracic Malignancy, Osaka Prefectural Medical Center for Respiratory and Allergic Diseases,
3-7-1 Habikino,
Habikino, Osaka 583-8588, Japan

Y. Kishi · Y. Fujii · R. Uehara
Medical & Biological Laboratories, Co., Ltd.,
4-5-3, Sakae, Naka-ku,
Nagoya 460-0008, Japan

Introduction

Lung cancer is the leading cause of death in adult men in Europe, the United States, and Japan. In 2010, approximately 157,300 Americans died of lung cancer from among 569,490 cancer deaths [1]. The exceptionally high mortality rate of lung cancer is, in part, due to the fact that lung cancer is often diagnosed at a late stage when the prognosis is usually poor, and early detection continues to be an elusive goal. For patients with advanced stage disease, modest but real improvements in overall survival and quality of life have been achieved with systemic chemotherapy [2]. However, the determination of efficacy of chemotherapy during the early phase of treatment is difficult to achieve. The decision whether to continue or to stop chemotherapy is traditionally guided by imaging-based tumor response evaluation, which is regarded as a surrogate marker of clinical benefit. Assessment by structural imaging has known limitations and also may have a poor correlation with pathologic response in non-small cell lung cancer [3]. On the other

hand, tumor markers that are currently available for lung cancer such as carcinoembryonic antigen (CEA), serum cytokeratin 19 fragment (CYFRA 21-1) and progastrin-releasing peptide (pro-GRP) are not satisfactory for diagnosis at an early stage or for monitoring the disease because of their relatively low sensitivity and specificity in detecting the presence of cancer cells [4–6]. Therefore, the identification of novel diagnostic and prognostic biomarkers for treatment response is eagerly desired.

Human epididymis protein 4 (HE4) was first identified in the epithelium of the distal epididymis and originally predicted to be a protease inhibitor involved in sperm maturation [7, 8]. Regarding malignant neoplasms, gene expression profiling studies have identified upregulation of HE4 in ovarian cancer [9–14], and several studies have shown HE4 protein expression in ovarian cancer, providing the opportunity for its application in histopathologic diagnosis [15–18]. Recent studies have revealed elevated HE4 protein levels in serum from ovarian cancer patients [19]. Moreover, HE4 protein expression was analyzed in other neoplasms including lung cancer [20, 21]. In this study, we developed novel enzyme-linked immunosorbent assay (ELISA) system to detect serum HE4, and by using this system, we showed that HE4 has potential for diagnostic marker of lung cancer. Specifically, we found that HE4 level after chemotherapy is strongly correlated with survival after the treatment.

Materials and methods

Patients and controls for measurement of HE4

Serum samples were collected from 49 consecutive patients with lung cancer (33 with adenocarcinoma, six with squamous cell carcinoma, one with large cell carcinoma and nine with small cell carcinoma), 18 with ovarian cancer, 10 with gastric cancer and eight with colon cancer. For control, we used 37 healthy adults (Table 1). The age range in 37 healthy control subjects was between 24 and 65 years. The age range in 49 lung cancer patients was between 40 and 78 years. We obtained written and oral informed consent from all participants. This study was approved by our institutional review board (IRB).

Patients for evaluation of chemotherapy

This prospective, IRB-approved study included 24 patients enrolled between 28 April 2008 and 26 August 2008. Patient characteristics are presented in Table 2. The median age was 69 years (45–76 years). All patients received chemotherapies. Specific regimens are presented in Table 2. Computed tomography (CT) scans were performed after 2 cycles of chemotherapy or 1 month of gefitinib/erlotnib therapy. All patients had measurable disease. Response categories were defined according to the Response Evaluation Criteria in Solid Tumors (RECIST) as complete response (CR), partial response (PR), stable disease (SD) and progressive disease (PD).

Cell lines

Nonsmall cell lung cancer cell lines A549, NCI-H1793, LU61, PC14, PC14PE6, PC9, SKLU1 and SKMES2; breast cancer cell line MCF7; colon cancer cell lines LOVO and WiDr; gastric cancer cell lines GC1Y, GT3TKB, HGC27, KATO3, MKN45 and OCUM1; pancreatic cancer cell line Miapaca2; prostate cancer cell lines 22Rv1 and PC3; and bladder cancer cell line T24 were cultured in DMEM medium (Sigma, St Louis, MO) supplemented with 10% fetal bovine serum (Equitech Bio Inc., Kerrville, TX). Non-small cell lung cancer cell line A427 was cultured in E-MEM medium (Sigma) supplemented with 10% fetal bovine serum. Non-small cell lung cancer cell lines NCI-H226, NCI-H358, NCI-H520, NCI-H522, NCI-H596, NCI-H2170, LC174, LC319 and ChagoK1; small cell lung cancer cell line DMS114; gastric cancer cell lines SCH, MKN74 and MKN1; pancreatic cancer cell lines KLM1, PK59 and PK1; and breast cancer cell line T47D were cultured in RPMI (Sigma) supplemented with 10% fetal bovine serum.

Table 1 Serum concentrations of HE4 in cancer patients and controls

Diagnosis	Number of study participants	HE4 (ng/ml)			Positive ratio (%)
		Mean (SD)	Median	Range	(Cutoff 6.56 ng/ml)
Lung cancer	49	14.0 (9.5)	11.4	4.3–63.4	89.8
NSCLC	40	13.3 (6.5)	11.4	4.3–30.7	90.0
SCLC	9	17.3 (18.1)	11.4	5.5–63.4	88.9
Ovarian cancer	18	10.9 (13.6)	6.1	2.0–60.2	44.4
Gastric cancer	10	7.2 (4.4)	7.1	2.1–17.4	60.0
Colorectal cancer	8	7.7 (3.5)	7.1	3.0–12.2	62.5
Normal	37	2.7 (1.2)	2.4	1.3–5.8	

Table 2 Patient characteristics

Characteristics	Number of patients
Gender	
Males/females	16/8
Age (years)	
<71/>71	13/11
Stage	
3A/3B/4	4/5/15
Tumor histology	
Adenocarcinoma	15
Squamous	4
Unclassified NSCLC	1
Small	4
Chemotherapy	
NSCLC	
Carboplatin + paclitaxel	5
Vinorelbine	3
Irinotecan	3
Cisplatin + gemcitabine	2
Gefitinib	2
Erlotinib	2
Carboplatin + gemcitabine	1
Cisplatin + vinorelbine	1
Gemcitabine	1
SCLC	
Carboplatin + etoposide	2
Cisplatin + etoposide	1
Cisplatin + irinotecan	1
Clinical response	
NSCLC	
CR/PR/SD/PD	0/5/10/5
SCLC	
CR/PR/SD/PD	0/3/1/0

Culture supernatants were collected at 5 to 6 days after cultivation and stored at 4°C until test.

Antigen preparation

Recombinant human HE4 protein was produced by amplifying the part coding for amino acids 1–124 from the cDNA encoding the transcript for human HE4 (Genbank accession no. NM_006103) with DNA polymerase (recombinant Taq polymerase; Takara Bio Inc., Shiga, Japan) and using the primers 5′-CGGGATCCGAGAAGACTGGCGTGTGCCCCG-3′ and 5′-TTTAAAGCGGCCGCTCAGAAATTGGGAGTGACA CAGG-3′. The amplified DNA was inserted into the *Bam*HI/*Not*I site of a mammalian expression plasmid DNA vector pSecTag2/Myc-His (Invitrogen, Carlsbad, CA) and transfected into HEK 293 T cells by lipofection (Lipofectamine 2000; Invitrogen). The culture supernatant of the transfectant was recovered at 5 days after lipofection and applied to a TALON resin to purify the secreted His-tagged proteins according to the manufacturer's instructions (Takara). The purified HE4 protein thus obtained was dialyzed with 4.0 l of PBS twice and kept frozen at −80°C until use as an immunogen or as a standard polypeptide for sandwich ELISA. Purity of the recombinant HE4 was confirmed by Coomassie Brilliant Blue (CBB) staining after electrophoresis under reduced condition (Fig. 1a).

Membrane-bound form of HE4 was constructed by molecular fusion together with the transmembrane region of a type I cell surface protein HIDE1 (accession number: A8MVS5) as briefly described below. Membrane-bound form of HE4 was produced by amplifying the part coding for amino acids 1–125 and 114–164 from the cDNAs of HE4 gene and HIDE1 gene, respectively, and both amplified DNAs were inserted into the *Xba*I site of pcDNA3.1/myc-His. *IRES-GFP* gene (Cell Biolabs, Inc., San Diego, CA) was then inserted into the *Pme*I site of the same plasmid DNA. The plasmid DNA was transfected into HEK 293 T cells, and GFP-positive cells were accounted for the cells expressing membrane bounded HE4.

Immunogen to develop a polyclonal antibody to human HE4 was prepared as follows. The part coding for amino acids 31–124 of the HE4 cDNA was ligated to the *Eco*RI/*Xho*I site of a bacterial expression vector pET28a (Novagen, Madison, WI). BL21 (DE3) competent cell (Takara) was transformed with the pET28a plasmid and cultured in LB medium. After induction of expression of HE4 protein using IPTG, the bacteria was collected and lysed with PBS containing 8 M urea, 1% NP-40, 0.5 mM PMSF and protease inhibitor cocktail (Sigma, St. Louis, MO). After centrifugation at 13,000*g* for 15 min, the supernatant containing His-tagged HE4 protein was loaded on a TALON resin, and the recombinant HE4 was eluted from the resin with 200 mM imidazole solution according to the manufacturer's instructions (Takara).

Antibody generation

To generate monoclonal antibodies against human HE4, 4-week-old BALB/c mice were immunized intraperitoneally with the recombinant HE4 produced from 293 T transfectant on days 0, 7, 14 and 16 (10 μg/shot). Following the last immunization, lymphocytes of the spleen were collected and fused with P3U1 myeloma cells in a 50% polyethylene glycol 4000 solution (Wako, Osaka, Japan) on day 18. The fused cells were plated on 96-well plates with RPMI-1640 medium containing 15% fetal calf serum (Equitech-Bio), penicillin/streptomycin (Invitrogen, Carlsbad, CA) and HAT solution (Invitrogen). After 10 days of incubation at 37°C with 5% CO_2 in a humidified environment, culture supernatants were collected and screened for their ability to bind to the immunogen by ELISA using recombinant HE4. Selected positive hybridoma colonies were expanded and

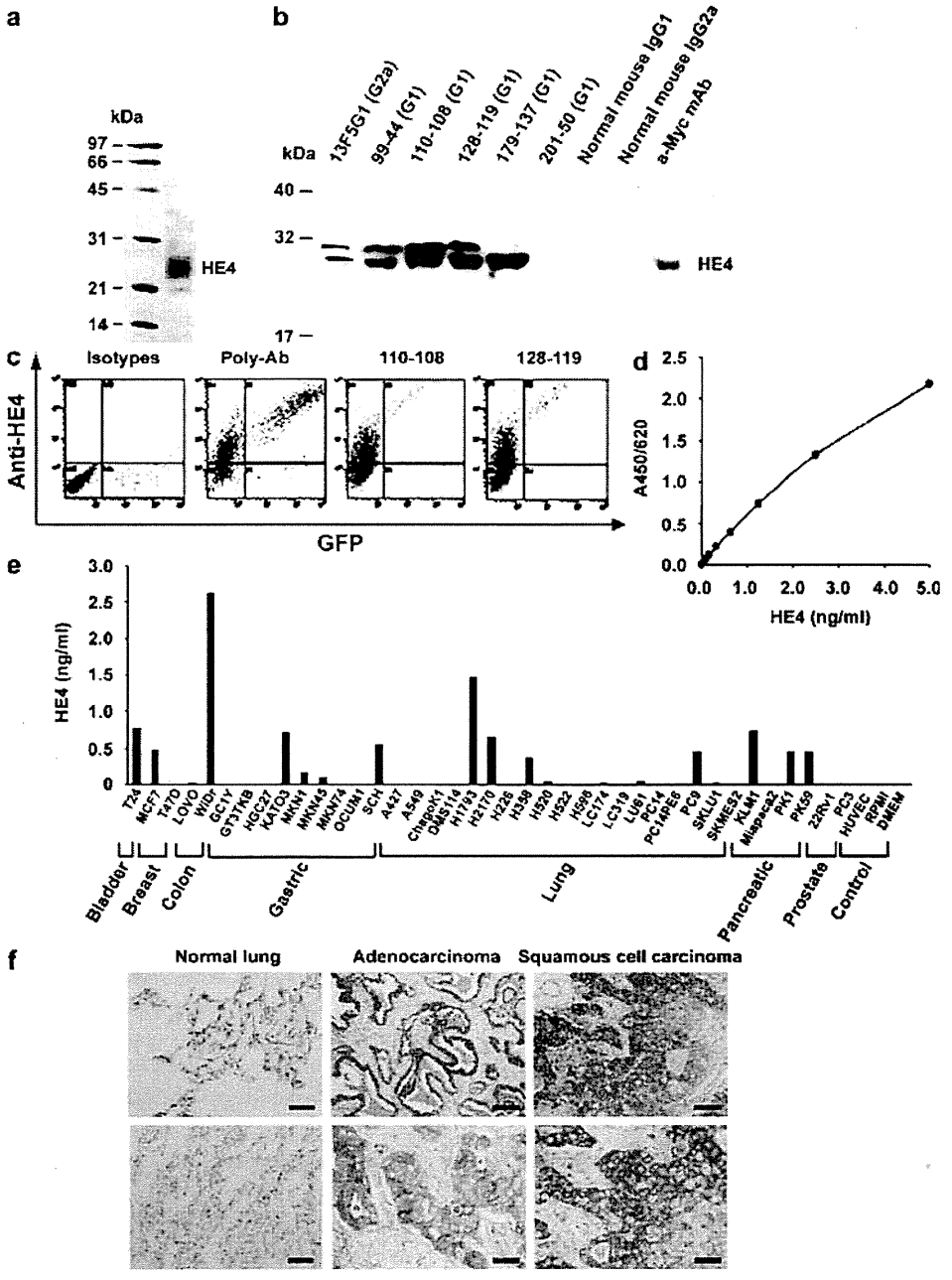

Fig. 1 **a** Purity of the prepared recombinant HE4 proteins for immunization. Proteins were electrophoresed under reduced condition and stained with Coomassie Brilliant Blue. **b** Reactivity of anti-HE4 antibodies to recombinant HE4 protein. Anti-HE4 antibodies were used for immunoprecipitation. Recovered proteins were separated by SDS-PAGE and electrotransferred to polyvinylidenefluoride (PVDF) membranes. Membranes were probed with anti-myc antibody for myc-His tagged HE4. Recombinant HE4 protein was applied for positive control. **c** Expression of HE4 on the surface of HE4-transfected 293 T cells. 293 T cells were incubated with anti-HE4 antibodies (110-108 and 128-119) or an isotype-matched control antibody and followed by PE-conjugate anti mouse IgG. Antigen expression was detected by flow cytometry. **d** Standard curves for HE4 in sandwich ELISA. ELISA displaying the mean absorbance values from indicated concentrations of recombinant proteins. **e** HE4 levels in the supernatants of cell lines measured by specific ELISA systems. **f** Immunohistochemical analysis of HE4 in lung cancer tissue. *Scale bar upper panels* 100 μm, *scale bar lower panels* 50 μm

subcloned by limiting dilution. An isostrip kit (Hoffmann-La Roche, Basel, Switzerland) was used for antibody isotype determination according to the manufacturer's instructions. Antibody purification was carried out with protein A affinity chromatography (GE Healthcare, Buckinghamshire, UK). Following a competition assay for the immunogen among the clones thus obtained (data not shown), clone 110-108 (IgG1) and clone 128-119 (IgG1) were selected to construct a sandwich ELISA for the detection of HE4.

Polyclonal antibody to recombinant human HE4 was prepared by injecting Japanese white rabbits (Kitayama Labs, Nagano, Japan) with purified HE4 (100 μg/injection) from *E. coli* subcutaneously in complete Freund's adjuvant followed by subsequent boosts in incomplete Freund's (Sigma). The serum was collected and IgG-purified with Protein G Sepharose (GE Healthcare).

Flow cytometry

At 24 h after transfection of the plasmid DNA-encoding membrane-binding HE4 into 293 T cells, the transfectant was treated with PBS containing 5 mM EDTA for 3 min to

detach from the culture dish, washed with PBS twice and incubated with 1 μg/ml of anti-HE4 antibodies or isotype-matched control for 30 min at 4°C in PBS containing 0.5% BSA and 2 mM EDTA. Following washing with the above buffer twice, PE conjugate antimouse IgG (MBL, Nagoya, Japan) for monoclonal antibody and PE-conjugated anti-rabbit polyclonal antibody (MBL) were added and further incubated for 30 min at 4°C. All flow cytometry was performed on Cytomics FC500 (Beckman Coulter, Fullerton, CA).

Immunoprecipitation and Western blot

The reactivity of anti-HE4 antibodies to recombinant HE4 protein was confirmed by immunoprecipitation. Fifteen microliters of Protein G sepharose suspended in PBS containing 0.01% BSA (Sigma) was incubated with 5 μg of anti-HE4 antibodies for 2 h at 4°C with gentle rocking. During this step, 250 ng of the recombinant myc-His-tagged HE4 protein was incubated with Protein G beads for 30 min at 4°C with shaking to preclear the samples. The Protein G Sepharose incubated with the antibodies were centrifuged at 1,000*g* for 2 min and washed with PBS three times. Then, the precleared samples were added to the tube containing the washed Protein G sepharose and rotated overnight at 4°C. After the incubation, the beads were washed with PBS three times and boiled in 25 μl of 2× Laemmli's SDS sample buffer for 5 min. Proteins (20 μl of sample per lane) were separated by sodium dodecylsulfate-polyacrylamide gel electrophoresis (SDS-PAGE) on a 12.5% polyacrylamide gel and electrotransfered to a polyvinylidenefluoride (PVDF) membrane. The membrane blocked with 5% nonfat milk in PBS containing 0.05% Tween 20 (blocking buffer) was incubated with 1.0 μg/ml mouse monoclonal anti-Myc antibody (MBL) to react with the precipitated Myc-His-tagged HE4 for 1 h at room temperature. After three washes with PBS containing 0.05% Tween 20, the membrane was incubated with a horseradish peroxidase (HRP)-conjugated antimouse IgG (MBL) diluted 1:5,000 with the blocking buffer. Chemiluminescence was developed according to the manufacturer's procedure (ECL; GE Healthcare).

Sandwich ELISA

The concentration of HE4 in culture media of cancer cell lines and donor sera was measured by a HE4-specific sandwich ELISA constructed as follows: 96-well microtiter plates (Nalge Nunc International Corp., Rochester, NY) were coated with the capturing antibody clone 110-108 with carbonate buffer at 4°C overnight. The plates were blocked with 200 μl PBS containing 1.0% BSA for 2 h and then incubated for 1 h with culture media diluted to 1:2 with sample diluent which consists of PBS containing 1.0% BSA and 0.1% Tween 20 or serum samples diluted to 1:10 with the same diluent and HRP-conjugated antibody 128-119 diluted to 1:140,000 with PBS containing BSA. After washing the plates with PBS containing Tween20, 100 μl/well TMB (Moss Inc., Pasadena, MD) was added, and the plates were incubated for 30 min at room temperature. The color development was stopped by the addition of H_2SO_4. Color intensity was determined at a wavelength of 450 nm with a reference wavelength of 620 nm. Analyte concentrations were calculated by referring to the standard curve using serial diluted recombinant HE4 (Fig. 1d).

Immunohistochemistry

Paraffin-embedded cancer tissue slices or noncancer tissue slices derived from lung cancer patients (adenocarcinoma and squamous cell carcinoma) were purchased from Outdo, Shanghai, China. The tissue slices were deparaffinized by treatment with xylene for 5 min three times, 100% ethanol for 5 min twice, 90% ethanol for 5 min once, 80% ethanol for 5 min once, 70% ethanol for 5 min once and PBS for 5 min three times. Subsequently, for an antigen retrieval, the specimens were immersed in a citrate buffer and heated by microwave for 10 min twice. In order to inactive the endogenous peroxidase activity, the specimens were then treated with PBS containing a 3% hydrogen peroxide solution at room temperature for 10 min. After washing with PBS twice, the specimens were blocked with blocking buffer and incubated with a blocking buffer containing 1 μg/ml of polyclonal HE4 antibody for 1 h at room temperature. After washing with PBS twice, the specimens were incubated with HRP-conjugated second antibody (EnVision Dual Link, Dako, Denmark) for 1 h at room temperature. Subsequently, the specimens were washed with PBS twice and allowed to react with a DAB chromogen (Dako) for 10 min at room temperature. The reaction was stopped by washing with water. After counterstaining with hematoxylene, the tissue slices were dehydrated with ethanol and xylene and made into specimens using a mounting medium (Matsunami Glass, Osaka, Japan).

Statistical analysis

To test for statistically significant differences between two groups, an unpaired Student's *t*-test was used. For comparisons among three or more groups, the values were analyzed by one-way ANOVA followed by Scheffe's post hoc comparisons. Differences were considered significant at $P<0.05$. For drawing of receiver operating characteristic (ROC) curves and estimation of the area under the ROC curve (AUC) statistics software SPBS (Comworks, Saitama, Japan) was used to quantify the ability to differentiate between

healthy volunteers and patients with lung cancer. Analyses of the prognostic impact of serum HE4 levels on survival from response evaluation to death or last follow-up used the Kaplan–Meier method and logrank test.

Results

Generation of ELISA specific for HE4

To generate monoclonal antibodies that specifically react with HE4, recombinant HE4 protein corresponding to the amino acids 1–124 of the transcript for human HE4 was produced by 293 T transfectants (Fig. 1a) and immunized to BALB/c mice. Supernatants of obtained hybridomas were tested for binding activity to microplates coated with immunizing antigen and further examined by a competition assay for the immunogen (data not shown). The specific reactivities of selected clone 13F5G1, 99-44, 110-108, 128-119, 179-137 and 201-50 to HE4 were checked by immunoprecipitation using myc-His-tagged recombinant HE4 (Fig. 1b). The specificity of 110-108 and 128-119 to HE4 was tested using the 293 T transfectant-expressing HE4 by flowcytometory. Clones 110-108 and 128-119 detected the antigen on the cell surface of 293 T transfectant (Fig. 1c). A sandwich ELISA for HE4 was constructed using the anti-HE4 antibodies 110-108 and 128-119. The standard curve using purified recombinant HE4 is shown in Fig. 1d. The HE4 sandwich ELISA detected the antigen in the culture supernatant of the various types of cancer cell lines (Fig. 1e). We investigated immunohistochemical staining of lung cancer tissue using anti-HE4 antibody. HE4 expression was detected in lung cancer tissues but not in normal lung tissues. We compared HE4 staining between adenocarcinoma and squamous cell carcinoma lung tissue samples but could not detect significant differences in staining intensity. Furthermore, we could not find a correlation between differentiation and HE4 staining of lung cancer tissues. Strong HE4 staining was

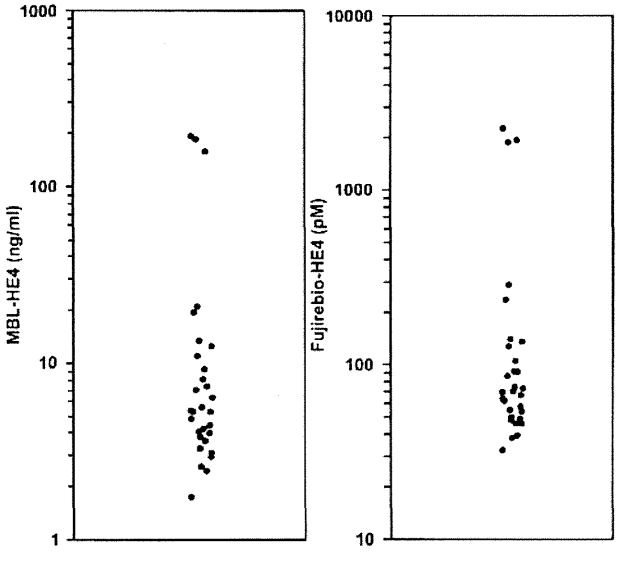

Fig. 2 HE4 levels in sera of ovarian cancer patients. HE4 levels determined by our ELISA system (*left*) and Fujirebio commercial ELISA kit (*right*). Each *dot* represents one patient

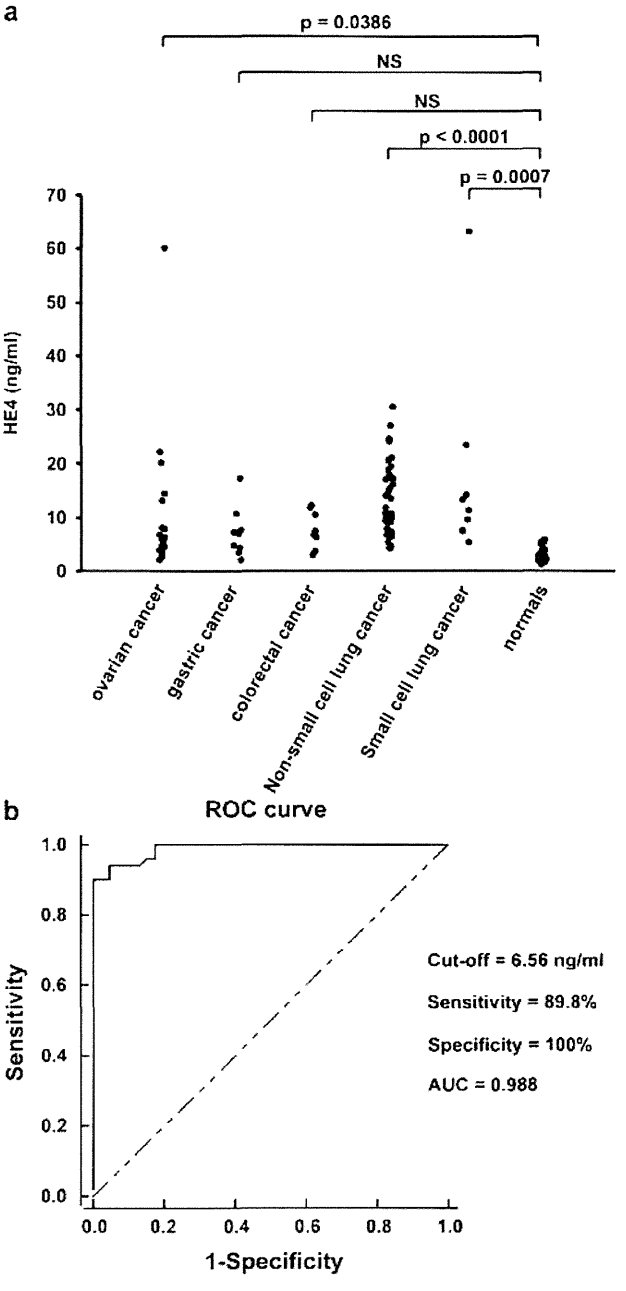

Fig. 3 a HE4 levels in the sera of cancer patients and normal controls. Each dot represents one patient. *NS* no significant. b Receiver operating characteristic (ROC) curves for HE4 for differentiation between lung cancer and healthy volunteers. The tables show the best statistical cutoff values for HE4 with pairs of sensitivity and specificity

Table 3 Pre- and post-treatment HE4 in lung cancer patients

Clinical response	Number of patients	Pre-treatment HE4 (ng/ml)			Post-treatment HE4 (ng/ml)		
		Mean (SD)	Median	Range	Mean (SD)	Median	Range
PR	8	23.0 (26.3)	14.2	8.3–86.5	12.6 (2.8)	12.9	8.2–16.1
SD	11	22.2 (32.3)	11.4	3.7–116.6	28.3 (44.4)	14.2	3.7–158.1
PD	5	21.3 (7.3)	22.8	9.3–28.1	23.8 (5.9)	25.9	14.2–29.1

detected in cytoplasmic and plasma membrane areas but not in nuclear area (Fig. 1f).

Evaluation of ELISA system

To assess the clinical potential of our ELISA system, we compared our ELISA system with an existing commercial ELISA kit (Fujirebio Diagnostics, Malvern, PA). We set the cutoff point of the existing ELISA kit as 150 pM based on the manufacturer's instructions (94.4 percentile of healthy individuals). In accordance with the existing ELISA kit, we set the cutoff point of our ELISA system as 5.5 ng/ml based on 94.4 percentile of 37 healthy individuals. We measured concentrations of HE4 of ovarian cancer patients by using two ELISA and found that our ELISA system shows better sensitivity for diagnosis of ovarian cancer than the existing ELISA kit by Fisher's exact probability test ($p<0.05$) (Fig. 2).

Diagnostic value of HE4

We measured serum HE4 levels in cancer patients and healthy controls by using our ELISA system. Mean serum HE4 levels in patients with non-small cell lung cancer, small cell lung cancer, ovarian cancer, gastric cancer, colorectal cancer and healthy adults were 13.3 ng/ml, 17.3 ng/ml, 10.9 ng/ml, 7.2 ng/ml, 7.7 ng/ml and 2.7 ng/ml (Table 1). Serum HE4 levels were significantly higher for non-small, small cell lung cancer and ovarian cancer patients than for healthy controls ($p<0.0001$, $p=0.0007$, and $p=0.0386$, respectively) (Fig. 3a).

To assess the clinical potential of HE4, we calculated sensitivities and specificities of HE4. The operating characteristics for HE4 with its cutoff points for achieving the best individual accuracy are shown in Fig. 3b. The AUC for serum HE4 was 0.988 for differentiating lung cancer patients from healthy adults, with a cutoff value of 6.56 ng/ml (sensitivity= 89.8%, specificity=100%) (Fig. 3b). Serum HE4 levels were elevated in 36/40 (90.0%) non-small cell lung cancer patients, 8/9 (88.9%) small cell lung cancer patients, 8/18 (44.4%) ovarian cancer patients, 6/10 (60.0%) gastric cancer patients and 5/8 (62.5%) colorectal cancer patients (Table 1). These results suggest that the sensitivity of HE4 was high in lung cancer patients.

Prognostic value of HE4

Pre- and post-treatment mean HE4 were 23.0 ng/ml (range 8.3–86.5 ng/ml) and 12.6 ng/ml (range 8.2–16.1 ng/ml), respectively, for PR patients, whereas 21.3 ng/ml (range 9.3–28.1 ng/ml) and 23.8 ng/ml (range 14.2–29.1 ng/ml), respectively, for PD patients (Table 3). Post-treatment mean

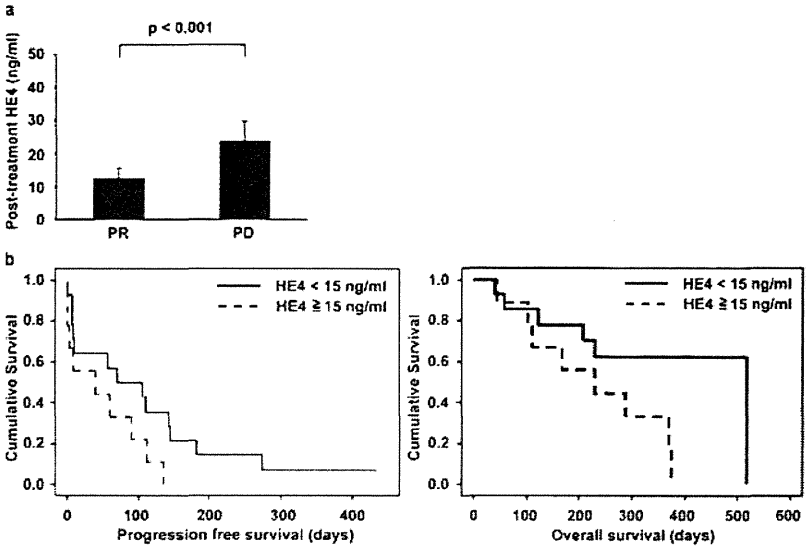

Fig. 4 **a** Post-treatment serum HE4 levels of lung cancer patients receiving chemotherapy. Figures show the average (*columns*) + SD (*bars*). **b** Kaplan–Meier plots of overall survival (*right*) and progression-free survival (*left*) after chemotherapy

HE4 in PR patients was significantly lower than that in PD patients ($p<0.001$) (Fig. 4a). Overall median survival after treatment was 9.6 months. Post-treatment HE4 levels were above the cutoff limit (15 ng/ml) in one of eight for PR and in four of five for PD patients. We divided patients into high (>15 ng/ml) and low (<15 ng/ml) HE4 groups post-treatment. We set the cutoff point at 15 ng/ml based on the median value of HE4 levels. Median overall survival of low HE4 group was significantly longer than that of high HE4 group (17.3 vs. 7.7 months; $p<0.05$) (Fig. 4b). Median progression-free survival after chemotherapy for low HE4 group was 2.4 months, compared with 1.4 months for high HE4 group ($p=0.083$) (Fig. 4b).

Discussion

In our study, we developed a novel ELISA system to detect serum HE4, and by using this system, we show that HE4 has potential as a diagnostic marker of lung cancer. Specifically, we found that serum HE4 levels in lung cancer patients after chemotherapy is strongly correlated with survival after the treatment.

Our HE4 ELISA shows better sensitivity for diagnosis of ovarian cancer than the existing HE4 ELISA kit. Furthermore, there are two advantages to our HE4 ELISA over the existing HE4 ELISA kit. First, while the existing ELISA kit is designed to use undiluted serum as the test sample, using our system, a small sample volume can be applied to our ELISA to detect HE4 in human serum. A diluted sample, maximally five times dilution, can be used in our assay system. This is of practical importance when simultaneous measures of other biomarkers are required from one serum sample. Second, a simpler and more rapid test is achieved using our HE4 ELISA. Test duration for our HE4 ELISA is approximately half of the time required by the existing HE4 ELISA kit. The existing HE4 ELISA kit requires a shaking procedure during reaction of antibody to the sample, while our new ELISA incubates the sample with antibody in a stationary condition. Thus, our HE4 ELISA does not require the purchase of specialized equipment for shaking incubation.

We evaluated the diagnostic efficacy of HE4 in lung, ovarian, gastric and colorectal cancer patients and found that HE4 indicated high sensitivity in lung cancer patients. Tissue expression of HE4 has been reported to be increased in pulmonary, ovarian and gastrointestinal carcinomas [15–18, 20, 21]. HE4 as a serum marker was mainly investigated in ovarian cancer patients and was shown to be a promising diagnostic marker [22]. We show that serum HE4 levels were significantly higher for not only ovarian cancer but also lung cancer patients than for healthy controls. Escudero et al. previously measured HE4 concentrations in patients with various types of malignant diseases and found that HE4 concentrations were abnormal primarily in gynecologic cancer and lung cancer [23]. Taken together, these data HE4 may be considered to be a potential diagnostic marker of lung cancer.

In this study, we found that post-treatment HE4 level is correlated with survival after chemotherapy. It was reported that high levels of serum HE4 is significantly correlated with worse prognosis in epithelial ovarian cancer patients [24]. Yamashita et al. reported that HE4 expression by immunohistochemistry staining is significantly correlated with prognosis in lung adenocarcinoma patients [25]. There is a growing need for diagnostic tools to estimate the prognosis of the patient, to monitor the treatment course and to early detect the response to therapy, which would help to optimize disease management on an individual basis. Our results suggest that serum HE4 is a promising prognostic marker. To our knowledge, this is the first time that the potential prognostic impact of serum HE4 in lung cancer patients has been investigated. We are aware of the small cohort of patients in this study, and thus, further study by larger scale prospective trials will be needed.

In conclusion, we used ELISA systems developed by us to detect significant differences in the levels of serum HE4 between lung cancer patients and normal controls. In addition, it is suggested that HE4 is correlated with prognosis after chemotherapy. We are planning a further study to evaluate serum HE4 for a diagnostic and prognostic marker by larger scale of patients.

Acknowledgments We appreciate Shintaro Nomura (Nagahama Institute of Bio-Science and Technology, Shiga, Japan) for providing helpful comments on immunohistochemical analysis, Barry Ripley for outstanding editing of the manuscript and Masako Ikeda for their technical assistance. We wish to thank Y. Ito, N. Kawakami and Y. Kanazawa for their secretarial assistance. This work was supported by a grant-in-aid from the Ministry of Health, Labour and Welfare, Japan.

Conflict of interest None.

References

1. Jemal A, Siegel R, Xu J, Ward E. Cancer statistics, 2010. CA Cancer J Clin. 2010;60:277–300.
2. Fruh M. The search for improved systemic therapy of non-small cell lung cancer—what are today's options? Lung Cancer. 2011;72:265–70.
3. Martini N, Kris MG, Gralla RJ, Bains MS, McCormack PM, Kaiser LR, Burt ME, Zaman MB. The effects of preoperative chemotherapy on the resectability of non-small cell lung carcinoma with mediastinal lymph node metastases (n2 m0). Ann Thorac Surg. 1988;45:370–9.
4. Shinkai T, Saijo N, Tominaga K, Eguchi K, Shimizu E, Sasaki Y, Fujita J, Futami H, Ohkura H, Suemasu K. Serial plasma carcinoembryonic antigen measurement for monitoring patients with advanced lung cancer during chemotherapy. Cancer. 1986;57:1318–23.

5. Pujol JL, Grenier J, Daures JP, Daver A, Pujol H, Michel FB. Serum fragment of cytokeratin subunit 19 measured by cyfra 21-1 immunoradiometric assay as a marker of lung cancer. Cancer Res. 1993;53:61–6.
6. Miyake Y, Kodama T, Yamaguchi K. Pro-gastrin-releasing peptide (31-98) is a specific tumor marker in patients with small cell lung carcinoma. Cancer Res. 1994;54:2136–40.
7. Kirchhoff C, Habben I, Ivell R, Krull N. A major human epididymis-specific cDNA encodes a protein with sequence homology to extracellular proteinase inhibitors. Biol Reprod. 1991;45:350–7.
8. Kirchhoff C. Molecular characterization of epididymal proteins. Rev Reprod. 1998;3:86–95.
9. Wang K, Gan L, Jeffery E, Gayle M, Gown AM, Skelly M, Nelson PS, Ng WV, Schummer M, Hood L, Mulligan J. Monitoring gene expression profile changes in ovarian carcinomas using cDNA microarray. Gene. 1999;229:101–8.
10. Schummer M, Ng WV, Bumgarner RE, Nelson PS, Schummer B, Bednarski DW, Hassell L, Baldwin RL, Karlan BY, Hood L. Comparative hybridization of an array of 21,500 ovarian cDNAs for the discovery of genes overexpressed in ovarian carcinomas. Gene. 1999;238:375–85.
11. Hough CD, Sherman-Baust CA, Pizer ES, Montz FJ, Im DD, Rosenshein NB, Cho KR, Riggins GJ, Morin PJ. Large-scale serial analysis of gene expression reveals genes differentially expressed in ovarian cancer. Cancer Res. 2000;60:6281–7.
12. Ono K, Tanaka T, Tsunoda T, Kitahara O, Kihara C, Okamoto A, Ochiai K, Takagi T, Nakamura Y. Identification by cDNA microarray of genes involved in ovarian carcinogenesis. Cancer Res. 2000;60:5007–11.
13. Welsh JB, Zarrinkar PP, Sapinoso LM, Kern SG, Behling CA, Monk BJ, Lockhart DJ, Burger RA, Hampton GM. Analysis of gene expression profiles in normal and neoplastic ovarian tissue samples identifies candidate molecular markers of epithelial ovarian cancer. Proc Natl Acad Sci U S A. 2001;98:1176–81.
14. Shridhar V, Lee J, Pandita A, Iturria S, Avula R, Staub J, Morrissey M, Calhoun E, Sen A, Kalli K, Keeney G, Roche P, Cliby W, Lu K, Schmandt R, Mills GB, Bast Jr RC, James CD, Couch FJ, Hartmann LC, Lillie J, Smith DI. Genetic analysis of early- versus late-stage ovarian tumors. Cancer Res. 2001;61:5895–904.
15. Schaner ME, Ross DT, Ciaravino G, Sorlie T, Troyanskaya O, Diehn M, Wang YC, Duran GE, Sikic TL, Caldeira S, Skomedal H, Tu IP, Hernandez-Boussard T, Johnson SW, O'Dwyer PJ, Fero MJ, Kristensen GB, Borresen-Dale AL, Hastie T, Tibshirani R, van de Rijn M, Teng NN, Longacre TA, Botstein D, Brown PO, Sikic BI. Gene expression patterns in ovarian carcinomas. Mol Biol Cell. 2003;14:4376–86.
16. Lu KH, Patterson AP, Wang L, Marquez RT, Atkinson EN, Baggerly KA, Ramoth LR, Rosen DG, Liu J, Hellstrom I, Smith D, Hartmann L, Fishman D, Berchuck A, Schmandt R, Whitaker R, Gershenson DM, Mills GB, Bast Jr RC. Selection of potential markers for epithelial ovarian cancer with gene expression arrays and recursive descent partition analysis. Clin Cancer Res. 2004;10:3291–300.
17. Drapkin R, von Horsten HH, Lin Y, Mok SC, Crum CP, Welch WR, Hecht JL. Human epididymis protein 4 (he4) is a secreted glycoprotein that is overexpressed by serous and endometrioid ovarian carcinomas. Cancer Res. 2005;65:2162–9.
18. Rosen DG, Wang L, Atkinson JN, Yu Y, Lu KH, Diamandis EP, Hellstrom I, Mok SC, Liu J, Bast Jr RC. Potential markers that complement expression of ca125 in epithelial ovarian cancer. Gynecol Oncol. 2005;99:267–77.
19. Hellstrom I, Raycraft J, Hayden-Ledbetter M, Ledbetter JA, Schummer M, McIntosh M, Drescher C, Urban N, Hellstrom KE. The he4 (wfdc2) protein is a biomarker for ovarian carcinoma. Cancer Res. 2003;63:3695–700.
20. Bingle L, Cross SS, High AS, Wallace WA, Rassl D, Yuan G, Hellstrom I, Campos MA, Bingle CD. Wfdc2 (he4): a potential role in the innate immunity of the oral cavity and respiratory tract and the development of adenocarcinomas of the lung. Respir Res. 2006;7:61.
21. Galgano MT, Hampton GM, Frierson Jr HF. Comprehensive analysis of he4 expression in normal and malignant human tissues. Mod Pathol. 2006;19:847–53.
22. Li J, Dowdy S, Tipton T, Podratz K, Lu WG, Xie X, Jiang SW. He4 as a biomarker for ovarian and endometrial cancer management. Expert Rev Mol Diagn. 2009;9:555–66.
23. Escudero JM, Auge JM, Filella X, Torne A, Pahisa J, Molina R. Comparison of serum human epididymis protein 4 with cancer antigen 125 as a tumor marker in patients with malignant and nonmalignant diseases. Clin Chem. 2011;57:1534–44.
24. Steffensen KD, Waldstrom M, Brandslund I, Jakobsen A. Prognostic impact of prechemotherapy serum levels of her2, ca125, and he4 in ovarian cancer patients. Int J Gynecol Canc. 2011;21:1040–7.
25. Yamashita S, Tokuishi K, Hashimoto T, Moroga T, Kamei M, Ono K, Miyawaki M, Takeno S, Chujo M, Yamamoto S, Kawahara K. Prognostic significance of he4 expression in pulmonary adenocarcinoma. Tumour Biol. 2011;32:265–71.

TOPICS

Serum leucine-rich alpha-2 glycoprotein is a disease activity biomarker in ulcerative colitis

Serada S, Fujimoto M, Terabe F, Iijima H, Shinzaki S, Matsuzaki S, Ohkawara T, Nezu R, Nakajima S, Kobayashi T, Plevy SE, Takehara T, Naka T

〔Inflamm Bowel Dis 2012；18：2169-2179 掲載〕

潰瘍性大腸炎の疾患活動性マーカーとしての血清ロイシンリッチアルファ2グリコプロテイン

世良田 聡* 藤本 穣* 仲 哲治*
Satoshi Serada Minoru Fujimoto Tetsuji Naka

Key words：炎症性腸疾患，潰瘍性大腸炎，バイオマーカー

論文の背景

炎症性腸疾患(inflammatory bowel disease：IBD)は再燃と寛解を繰り返す原因不明の慢性炎症性疾患であり，潰瘍性大腸炎(ulcerative colitis：UC)とクローン病(Crohn's disease：CD)に分類される．近年，IBDに対する免疫抑制薬，調節薬などを用いた治療法に加え，IBDの病態と関係の深いサイトカインの一つであるTNF-αを標的とした抗体医薬など生物学的製剤が使用され始めたことによって劇的な治療効果が発揮されたことにより，寛解を目指した治療が現実になりつつある[1),2)]．IBDの診療においては，内視鏡検査・X線検査などの画像診断，生検組織の病理学的診断といった炎症局所の評価が重要であることは明白であるが，これらの評価法以外にも，バイオマーカーの測定を併用することで炎症性腸疾患の診断や治療が低侵襲的，簡便で客観的，かつ低コストで行える可能性がある．

CDの疾患活動性を把握する活動性マーカーとしてはC-reactive protein(CRP)，赤沈検査(ESR)，白血球数などが知られている．これらの検査マーカーはCDの炎症局所である腸以外の炎症においても高値を示す．また，UCにおいてはこれらのマーカーはCDほど有用ではないといわれている[3)]．さらに，UCの疾患活動性を評価するために内視鏡的な所見は重要な情報であるが，内視鏡による検査は侵襲性が高いことが問題であり，短期間に繰り返して検査することが困難である．そのため，UCの治療に伴う疾患活動性の適切な評価を行うに当たり，侵襲性が少ない新規疾患活動性マーカーが必要とされている．

筆者らはこれまでにインフリキシマブ(TNF-α阻害抗体)治療前と治療後の関節リウマチ同一患者血清に対して定量的プロテオミクス手法を用

*独立行政法人医薬基盤研究所創薬基盤研究部免疫シグナルプロジェクト(〒567-0085 大阪府茨木市彩都あさぎ7-6-8)
* Laboratory for Immune Signal, National Institute of Biomedical Innovation, 7-6-8 Saito-Asagi, Ibaraki-city, Osaka 567-0085, Japan

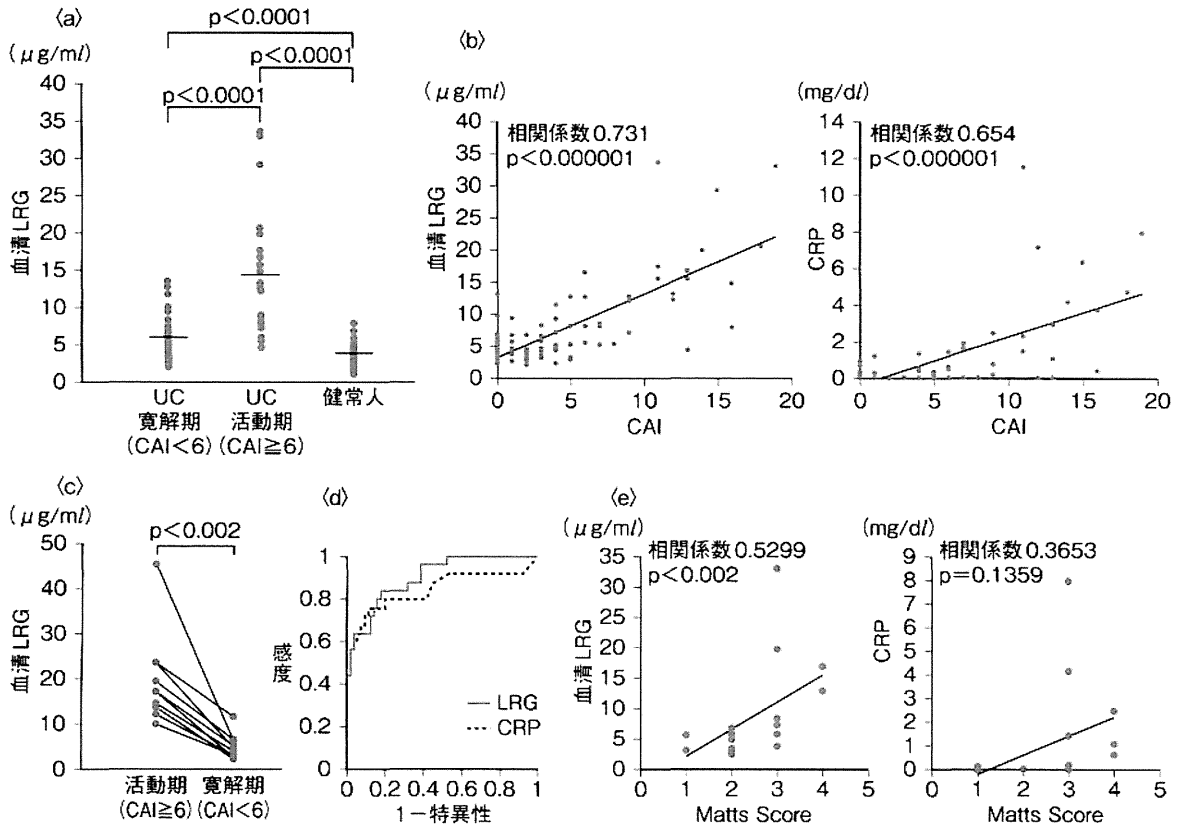

図　潰瘍性大腸炎の疾患活動性マーカーとしての leucine-rich α-2 glycoprotein (LRG) の有用性

a：潰瘍性大腸炎患者血清中の LRG 濃度
b：血清 LRG 濃度，および CRP と CAI との相関
c：活動期，寛解期における血清 LRG 濃度の変動
d：活動期と寛解期を区別する血清 LRG 濃度と CRP の ROC 曲線解析
e：血清 LRG 濃度，および CRP と内視鏡スコア (Matts Score) との相関
CAI：clinical activity index, ROC：receiver operating characteristic
〔Serada S, et al：Inflamm Bowel Dis 2012；18：2169-2179 より改変〕

いることで，治療によって発現変動を示す血清タンパク質を網羅的に探索した．その結果，CRP や serum amyloid A (SAA) のような既知の炎症マーカータンパク質のみならず，leucine-rich alpha-2 glycoprotein (LRG) というタンパク質が治療後よりも治療前にて高値を示すことを明らかにした[4]．LRG は 1977 年に発見された血清中に存在する糖タンパク質で，ロイシンリッチリピートと呼ばれる特徴的なドメインを八つ含むタンパク質であるが，生理的機能はまだ明らかにされていない[5]．疾患活動性マーカーとしての血清 LRG の有用性を検討するため，ELISA 法を用いて関節リウマチ患者血清中の LRG を定量した結果，LRG は関節リウマチの優れた疾患活動性マーカーとなりうることを明らかにした．さらに，血清 LRG が CD においても優れた疾患活動性マーカーとなりうることを明らかにしている．本論文は UC の疾患活動性マーカーとしての血清 LRG

の有用性について報告している.

論文の概要

UC患者82例を対象とし，血清中のLRG濃度をELISA法により定量した．その結果，血清LRG濃度は活動期(25例)において，寛解期(57例)，および健常人(50例)の血清LRG濃度よりも有意に高値を示した(図a)．UCの疾患活動性スコアであるClinical Activity Index(CAI)と血清LRG濃度との相関を解析した．その結果，血清LRG濃度はCRPよりもCAIと強く有意に相関した(図b)．さらに，寛解期の患者血清中のLRG濃度は活動期に比較して有意な低下を認めた(図c)．また，receiver operating characteristic (ROC)曲線解析から，UC活動期と寛解期を区別するマーカーとして血清LRG濃度はCRPよりも優れていた(図d)．UCの炎症の状態を把握するうえで内視鏡所見は直接的な指標となる．そこで，血清LRG濃度と内視鏡スコア(Matts Score)との相関を解析した．その結果，血清LRG濃度はCAIだけでなく内視鏡スコアに対してもCRPよりも強く相関関係を示した(図e)．また，LRGは炎症局所の腸組織において高発現することが免疫組織化学染色法にて確認された．LRGは正常腸組織からは発現がほとんどみられないものの，UC患者の炎症局所である腸組織において高発現するため，疾患活動性とより強く相関することが示唆されており，この点は炎症時に肝臓から産生されるCRPと異なった特徴と考えられる．

IL-6欠損マウスを用いて炎症性腸疾患モデルの血清LRG濃度を解析した．その結果，野生型マウス，IL-6欠損マウスのいずれにおいてもdextran sulfate sodium(DSS)誘導性腸炎を誘導することにより血清LRG濃度の上昇が野生型マウスとIL-6欠損マウスの間において同程度で認められた．このことから，LRGの発現にはIL-6が必ずしも必要ではないことが明らかとなり，従来の炎症マーカーとして使用されているCRPとは発現調節機序が異なることが判明した．

以上の結果，血清LRGはCRPとは異なるUCの新規疾患活動性マーカーとなりうることが明らかとなった．興味深いことに，血清LRGはIL-6非依存性の発現調節機序が存在する炎症マーカーとなりうる．このことより，IL-6阻害療法を受けるためCRP値が常に陰性化するため，CRPを疾患活動性マーカーや感染症検出マーカーとして使えない関節リウマチなどの自己免疫疾患患者において，LRGが疾患活動性マーカー，あるいは感染症を検出できる有用性の高いマーカーとなることが期待される．

文　献

1) Feagan BG, Reinisch W, Rutgeerts P, et al : The effects of infliximab therapy on health-related quality of life in ulcerative colitis patients. Am J Gastroenterol 2007 ; 102 : 794-802
2) Fiorino G, Peyrin-Biroulet L, Repici A, et al : Adalimumab in ulcerative colitis : hypes and hopes. Expert Opin Biol Ther 2011 ; 11 (1) : 109-116
3) Vermeire S, Van Assche G, Rutgeerts P : Laboratory markers in IBD : useful, magic, or unnecessary toys? Gut 2006 ; 55 : 426-431
4) Serada S, Fujimoto M, Ogata A, et al : iTRAQ-based proteomic identification of leucine-rich alpha-2 glycoprotein as a novel inflammatory biomarker in autoimmune diseases. Ann Rheum Dis 2010 ; 69 : 770-774
5) Haupt H, Baudner S : Isolation and characterization of an unknown, leucine-rich 3.1-S-alpha2-glycoprotein from human serum. Hoppe Seylers Z Physiol Chem 1977 ; 358 : 639-646

Key words : inflammatory bowel diseases, ulcerative colitis, biomarker

Journal of proteome research

Article

pubs.acs.org/jpr

Comprehensive Identification of Substrates for F-box Proteins by Differential Proteomics Analysis

Kanae Yumimoto,[†,‡] Masaki Matsumoto,[†,‡] Koji Oyamada,[†,‡] Toshiro Moroishi,[†,‡] and Keiichi I. Nakayama*[,†,‡]

[†]Department of Molecular and Cellular Biology, Medical Institute of Bioregulation, Kyushu University, 3-1-1 Maidashi, Higashi-ku, Fukuoka, Fukuoka 812-8582, Japan

[‡]CREST, Japan Science and Technology Agency (JST), Kawaguchi, Saitama 332-0012, Japan

Supporting Information

ABSTRACT: Although elucidation of enzyme–substrate relations is fundamental to the advancement of biology, universal approaches to the identification of substrates for a given enzyme have not been established. It is especially difficult to identify substrates for ubiquitin ligases, given that most such substrates are immediately ubiquitylated and degraded as a result of their association with the enzyme. We here describe the development of a new approach, DiPIUS (differential proteomics-based identification of ubiquitylation substrates), to the discovery of substrates for ubiquitin ligases. We applied DiPIUS to Fbxw7α, Skp2, and Fbxl5, three of the most well-characterized F-box proteins, and identified candidate substrates including previously known targets. DiPIUS is thus a powerful tool for unbiased and comprehensive screening for substrates of ubiquitin ligases.

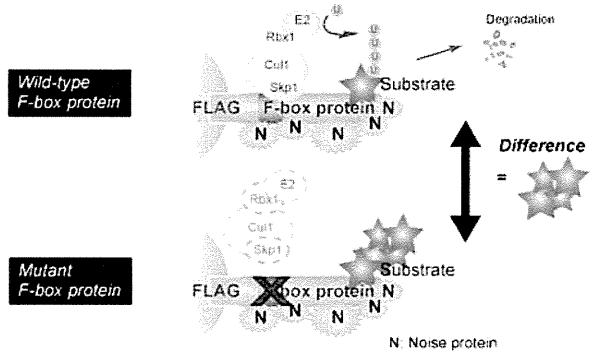

KEYWORDS: *ubiquitin ligase, F-box protein, substrate identification, differential proteomics*

INTRODUCTION

Enzyme–substrate relations have been discovered by substrate-to-enzyme approaches in most instances.[1−5] Analysis of the genome sequences of various organisms has led to the identification of large numbers of enzymes such as protein kinases[6] and ubiquitin ligases[7] on the basis of their conserved catalytic domains. However, universal approaches to the identification of substrates for a given enzyme have not been established to date, and many enzymes remain "orphans". One of the challenges to substrate identification is detection of the interaction between enzymes and substrates, which is generally weak and transient and has therefore been referred to as "kiss and run". Although recent advances in mass spectrometry (MS) have allowed the detection of such weak interactions, elimination of the large number of proteins that bind nonspecifically to a bait protein remains problematic. It is also difficult to apply this approach to the identification of substrates for ubiquitin ligases, given that the ubiquitylation of most such substrates by the ubiquitin ligase promotes their degradation by the 26S proteasome.[8]

The Skp1–Cul1–F-box protein (SCF) complex is one of the most well-characterized types of mammalian ubiquitin ligase. Each SCF complex is composed of four subunits: Skp1, Cul1, and Rbx1 (also known as Roc1 or Hrt1) as invariable components and an F-box protein that primarily determines substrate specificity as a variable component.[9−11] Cul1 serves as a scaffold and interacts via its COOH terminus with the RING-finger protein Rbx1 to recruit a ubiquitin-conjugating enzyme, whereas its NH_2 terminus interacts with Skp1, an adaptor protein that binds to the F-box domain of an F-box protein, which in turn is responsible for substrate specification. The substrate specificity of each SCF complex is thus conferred by the incorporated F-box protein, with each such protein recognizing a different group of substrates. F-box proteins constitute a large family of eukaryotic proteins, with ~70 F-box proteins having been identified in humans.[12] Whereas some F-box proteins have been found to contribute to cellular activities such as cell cycle progression,[9] synapse formation,[13,14] plant hormone responses,[15] and the circadian clock,[16−18] the functions of most F-box proteins remain to be elucidated because their substrates are unknown.

We now describe the development of a general approach to the identification of substrates for SCF type ubiquitin ligases. The application of this approach, designated DiPIUS (differential proteomics-based identification of ubiquitylation substrates), to Fbxw7α, Skp2, and Fbxl5 resulted in the identification of many candidate substrates. These candidates include previously known targets, providing support for the fidelity of this method. We propose DiPIUS as a powerful tool

Received: December 10, 2011
Published: April 23, 2012

for the discovery of substrates for any ubiquitin ligase in cases in which the ubiquitylation of the substrate is followed by proteasomal degradation.

MATERIALS AND METHODS

Cell Culture

HEK293T cells, Neuro2A cells, mHepa cells, and mCAT-HeLa cells (HeLa cells stably expressing mCAT1, a transporter for basic amino acids, as well as a receptor for ecotropic retrovirus infection)[19] were maintained in Dulbecco's modified Eagle's medium (DMEM) supplemented with 10% fetal bovine serum (FBS; Invitrogen), 1 mM sodium pyruvate, penicillin (100 U/mL), streptomycin (100 mg/mL), 2 mM L-glutamine, and nonessential amino acids (10 mL/L; Gibco). The murine myoblast precursor cell line C2C12 was maintained in DMEM supplemented with 10% FBS. Differentiation of C2C12 cells toward the myoblast lineage was induced by culture in DMEM supplemented with 0.1% FBS.

Antibodies

Antibodies to c-Myc (N-262) were obtained from Santa Cruz Biotechnology; those to Skp1, p27, and Hsp90 were from BD Biosciences; those to Cul1 were from Zymed; and those to the FLAG epitope (M2) were from Sigma.

Plasmids

Complementary DNAs encoding mouse Fbxw7α or its ΔF mutant were subcloned into p3 × FLAG-CMV 7.1 (Sigma). The resulting vectors were introduced into mCAT-HeLa cells with the use of the FuGENE 6 or FuGENE HD transfection reagents (Roche). For retroviral expression, cDNAs for FLAG-tagged mouse Fbxw7α, Skp2, or corresponding mutants were subcloned into pMX-puro (kindly provided by T. Kitamura). The resulting vectors were introduced into Plat E cells with the use of FuGENE HD. The recombinant retroviruses thereby generated were used to infect mCAT-HeLa, Neuro2A, C2C12, or mHepa cells, which were then subjected to selection in medium containing puromycin (10 μg/mL). Complementary DNAs for FLAG-tagged mouse Fbxl5 or its PE/AA mutant were subcloned into pMX-puro-CMV. The resulting vectors together with pCL-Ampho (IMGENEX) were introduced into HEK293T cells with the use of FuGENE HD, and the recombinant retroviruses thereby generated were used to infect HEK293T cells, which were then subjected to selection in medium containing puromycin (5 μg/mL). These latter cells were treated with ferric ammonium citrate (100 μg/mL) for 24 h before sample preparation.

SILAC

SILAC (stable isotopic labeling using amino acids in cell culture) labeling medium (KOHJIN-bio) lacking lysine and arginine was reconstituted and supplemented with 10% dialyzed FBS and amino acid stocks prepared in phosphate-buffered saline (PBS). We added $^{13}C_6$-lysine and $^{13}C_6$-arginine (Cambridge Isotope Laboratories) to heavy medium and normal lysine and arginine (Sigma-Aldrich) to light medium. mCAT-HeLa or HEK293T cells were cultured in heavy medium for at least six cell doublings to allow adaptation and full incorporation of the stable isotope-containing amino acids. The wild-type F-box protein was expressed in light-labeled cells and the mutant protein in heavy-labeled cells.

Immunoaffinity Purification

Wild-type Fbxw7α, Skp2, or Fbxl5 tagged with the FLAG epitope at its NH_2 terminus was expressed in light-labeled mCAT-HeLa cells or HEK293T cells, and the corresponding mutant protein was expressed in heavy-labeled cells, for DiPIUS. Cells were incubated for 6 h in the presence of the proteasome inhibitor MG132 (10 μM; Peptide Institute) and were then lysed in 8 mL of a lysis buffer containing 20 mM HEPES-NaOH (pH 7.5), 150 mM NaCl, 1% digitonin, 10 mM NaF, 10 mM $Na_4P_2O_7$, 0.4 mM Na_3VO_4, 0.4 mM EDTA, leupeptin (20 μg/mL), aprotinin (10 μg/mL), and 1 mM phenylmethylsulfonyl fluoride. The lysates were centrifuged at 2200g for 20 min at 4 °C to remove debris, and the resulting supernatants were adjusted with lysis buffer to achieve a protein concentration of 2.5 mg/mL. The supernatants (20 mg of protein in 8 mL of solution) from light-labeled cells and heavy-labeled cells were combined for DiPIUS and incubated for 1 h at 4 °C with 120 μL of beads conjugated with M2 antibodies to FLAG (Sigma). The beads were washed three times with 4 mL of a solution containing 10 mM HEPES-NaOH (pH 7.5), 150 mM NaCl, and 0.1% Triton X-100, and bead-bound proteins were then eluted with the FLAG peptide (500 μg/mL; Sigma), precipitated with ice-cold 20% trichloroacetic acid, and washed with acetone. The concentrated proteins were then digested with Lys-C and trypsin, and the resulting peptides were analyzed with a QSTAR Elite Hybrid LC–MS/MS system (Applied Biosystems) for DiPIUS of Skp2 or with an LTQ Orbitrap Velos LC–MS/MS system (Thermo Finnigan) for DiPIUS of Fbxw7α or Fbxl5. For DiPIUS-NL, the concentrated proteins derived separately from lysates of nonlabeled cells expressing the wild-type or mutant F-box proteins were dissolved in SDS sample buffer, fractionated by SDS–polyacrylamide gel electrophoresis (PAGE), and stained with silver. Individual lanes of the stained gel were sliced into 8–16 pieces, and proteins within these pieces were subjected to in-gel digestion with trypsin as described previously.[20] The resulting peptides were dried and then dissolved in a solution containing 0.1% trifluoroacetic acid and 2% acetonitrile before analysis with an ion-trap mass spectrometer (LTQ-XL, Thermo Finnigan). The high molecular weight fractions were excluded from the analysis.

Spectral Counting

Peak lists were generated by lcq_dta.exe (Thermo Finnigan) and were compared with the use of the MASCOT algorithm (ver. 2.2.1) either with the "Target-decoy" Human IPI version 3.1.6 database [date of release, November 2006; with 62322 target sequences, searched against a total of 124644 sequences (target and reverse/decoy)] or with the "Target-decoy" Mouse IPI version 3.4.4 database [date of release, June 2008; with 55078 target sequences, searched against a total of 110156 sequences (target and reverse/decoy)], both maintained by the European Bioinformatics Institute. Trypsin was selected as the protease, the allowed number of missed cleavages was set to one, and carbamidomethylation of cysteine was selected as the fixed modification. Oxidized methionine and pyroglutamine were searched as variable modifications. The precursor mass tolerance was 1.5 Da, and the tolerance of MS/MS ions was 0.8 Da. Assigned high-scoring peptide sequences (MASCOT score >35) were processed by in-house software. If the MASCOT score was <45 (peptides for which the MS2 score was above the 95th percentile of significance), assigned sequences were manually confirmed by comparison with the corresponding

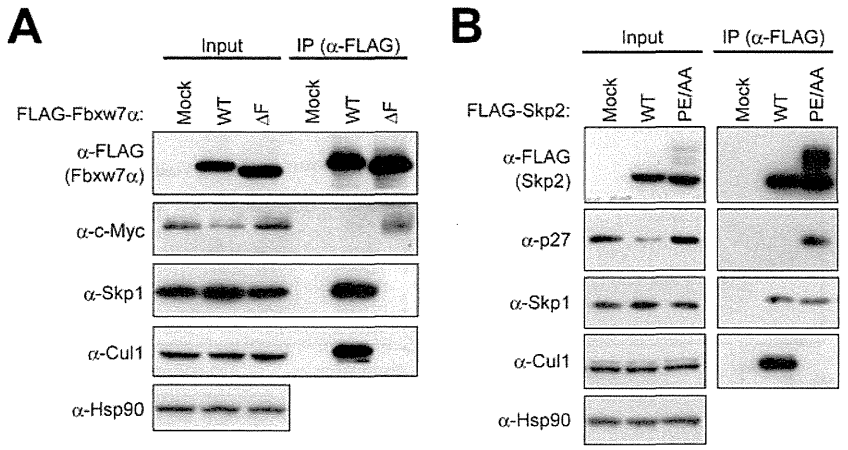

Figure 1. Stable interaction between mutant F-box proteins and their substrates. mCAT-HeLa cells transfected with expression vectors for FLAG-tagged wild-type (WT) or mutant (ΔF) Fbxw7α (A) or FLAG-tagged WT or mutant (PE/AA) Skp2 (B), or with the corresponding empty vector (Mock), were lysed and subjected to immunoprecipitation (IP) with antibodies to (α-) FLAG. The resulting precipitates as well as the original cell lysates (Input) were subjected to immunoblot analysis with the indicated antibodies.

collision-induced dissociation spectra on the basis of the following criteria: (i) a delta score of >15 or (ii) at least six successive matches for y- or b-ions or at least three blocks of three successive matches for y- or b-ions. Identified peptides from independent experiments were integrated and regrouped by IPI accession number. When multiple accession IDs were obtained with the same set of peptides, a representative IPI accession was chosen according to the following order of priorities: (i) IPI accession containing NCBI GeneID, (ii) IPI accession with the use of Swiss-Prot as the master sequence, and (iii) IPI accession with the use of TrEMBL as the master sequence. Proteins identified in only one experiment or with a single-peptide assignment were removed from spectral counting data. Estimated false discovery rates (FDRs) were zero at the protein level in all experiments with the exception of that involving the expression of Skp2 in mHepa cells (FDR = 0.26%) and that regarding the growth state of C2C12 cells (FDR = 0.51%). For derivation of the consensus Cdc4 phosphodegron (CPD) sequence, we aligned the CPDs of 16 known Fbxw7 (Cdc4) substrates in mammals or yeast[10] and found that positions −1 or +5 (or both) showed a preference for leucine or proline.

Quantification for SILAC

The peak lists were generated by Mascot Distiller (version 2.3.0) and compared with the "Target-decoy" Human IPI version 3.1.6 database with the use of the MASCOT algorithm (ver. 2.2.1). Trypsin was selected as the protease, the allowed number of missed cleavages was set to one, and carbamidomethylation of cysteine was selected as the fixed modification. Oxidized methionine, pyroglutamine, $^{13}C_6$-lysine, and $^{13}C_6$-arginine were searched as variable modifications. Precursor mass tolerance was 200 ppm for QSTAR Elite Hybrid and 20 ppm for LTQ Orbitrap Velos, and tolerance of MS/MS ions was 0.3 Da for QSTAR Elite Hybrid and 0.8 Da for LTQ Orbitrap Velos. Assigned high-scoring peptide sequences (MASCOT score >20) were processed by in-house software; the MASCOT score cutoff value for SILAC analysis was lower than that for spectral counting (MASCOT score >35) because of the use of high-resolution LC-MS/MS systems for SILAC. If the MASCOT score was <45, assigned sequences were manually confirmed as described above for spectral counting, and the FDR at the peptide level was estimated. SILAC quantitation was performed with the use of the Mascot Distiller Quantitation Tool (version 2.3.0). Extracted ion chromatogram (XIC) peak areas for the heavy and light peptides were measured, and the results were verified by manual inspection of MS spectra. SILAC ratios were calculated by comparison of the XIC peak areas of light peptides with those of the heavy peptides. The method "Auto" was selected for the removal of outlier peptide pairs (peptides with a number between 4 and 25 by Dixon's method or of >25 by Rosner's method). SILAC ratios for different peptides of a protein were averaged to give protein abundance ratios, which were then normalized with the heavy/light ratio for each bait protein (Fbxw7α, Skp2, or Fbxl5).

Functional Enrichment Analysis

We used a Web-based implementation of Database for Annotation, Visualization, and Integrated Discovery (DAVID)[21] for functional annotation of enriched proteins among specific binding proteins for each F-box protein and nonspecific binding proteins that interact with at least two of Fbxw7α, Skp2, and Fbxl5. We used the database of Gene Ontology (GO) level 2 for this analysis. Overrepresented functional categories among binding proteins were identified relative to the entire human genome with the use of Fisher's exact test. We processed the GO term lists with P values of <0.05 and contributing rate of proteins of >10%.

Immunoprecipitation and Immunoblot Analysis

Cells were incubated for 6 h in the presence of the proteasome inhibitor MG132 (10 μM) prior to harvest. Cell lysis and immunoprecipitation were performed as described.[22] Immunoprecipitates and cell lysates were subjected to immunoblot analysis as described,[23] with Hsp90 used as a loading control.

RESULTS

Development of the DiPIUS System

A substrate would be expected to be ubiquitylated and degraded on its recognition by a ubiquitin ligase, resulting in a decrease in its cellular concentration. In contrast, an F-box protein with a point mutation or deletion in the F-box domain might be expected to retain the ability to associate with a substrate but to have lost the ability to mediate ubiquitin conjugation, resulting in accumulation of the substrate in the

dx.doi.org/10.1021/pr201216u | J. Proteome Res. 2012, 11, 3175–3185